Numerical Analysis of Meso-scopic Failure Process in Concrete Model

Hokkaido University　○Student Member　Kouhei Nagai
Hokkaido University　Member　Yasuhiko Sato
Hokkaido University　Member　Tamon Ueda

1. INTRODUCTION

Concrete is a composite material consists of aggregate and mortar on meso level. Evaluation of fracture process on this level is useful to quantify concrete properties on macro level in which homogeneous is assumed. It is considered, furthermore, that influences of environmental action on mechanical characteristics of concrete can be clarified more precisely with using analytical approach on meso-scopic. Many experimental studies about fracture mechanism on meso level have been conducted so that major factors, such as existence of interfacial zone between aggregate and mortar, to fracture mechanics were reported. But numerical analysis of fracture process on meso level has not been carried out yet. In this study, numerical simulation of compressive test of simplified aggregate-mortar concrete model is conducted by Rigid Body Spring Method (RBSM). This analytical method is useful to simulate brittle behavior caused by crack localization. In this analysis, random shape elements are created in order to avoid formation of unarbitrary crack path. Fracture process and behavior of each component, aggregate, mortar and interface zone, are examined and stress-strain curves are compared with experimental results.

2. ANALYTICAL METHOD

A rigid body spring method is one of discrete approaches, was developed by Kawai[1]. Analytical model is divided into polygon elements interconnected along their boundaries by springs(Fig.1).

Each element has two translational and one rotational degrees of freedom defined at a certain point within its interior. The interface between two elements consists of two individual springs. Normal and shear springs are placed at the midpoint of the boundary. Since cracks initiate and propagate along boundaries between elements, mesh arrangement may affect fracture direction. It means that the crack pattern is strongly influenced by the local structure of the network. To avoid formulation of cracks with unarbitrary direction, a random geometry is introduced using a Voronoi diagram. The Voronoi diagram is the collection of Voronoi cells as shown in Fig.2. Each Voronoi cell represents aggregate or mortar element in the analysis. The Voronoi cell is constructed by a set of perpendicular bisectors of nuclei that are closer to the nucleus of the cell than all other nuclei (Fig.3). Since those nuclei are randomly generated, a random geometry of a rigid body spring network can be obtained.

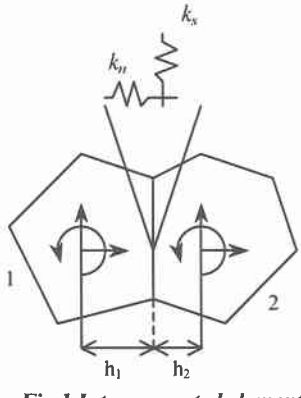

Fig.1 Interconnected elements

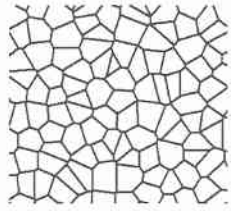

Fig.2 Voronoi diagram

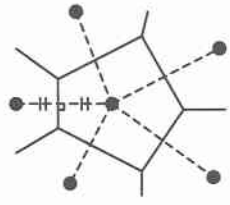

Fig.3 Voronoi cell

3. MATERIAL MODELS

Material characteristics of mortar and interface are represented by means of the modeling of springs. In normal springs compressive and tensile stresses (σ) are developed. Shear springs develops shear stress (τ). Aggregate model in this study is made of mortar not stone nor steel.

It is assumed in this study that softening behavior observed in experiments based on macroscopic doesn't exist. Therefore the following stress-strain curves without softening part are adapted as a constitutive law in the springs (see Fig.4).

$$\begin{aligned} &\sigma = E\varepsilon && (\sigma \geqq -3f_t) \\ &\sigma = -\left\{\left(-\frac{E\varepsilon}{f_t}-3\right)^{0.76}+3\right\}f_t && (\sigma < -3f_t) \\ &\tau = G\gamma \end{aligned} \qquad (1)$$

where E and G are Young's modulus and shear modulus, ε and γ are the strain of normal and shear springs, respectively. And f_t is tensile stress. Equation(1) was derived by comparing with the experimental results[2].

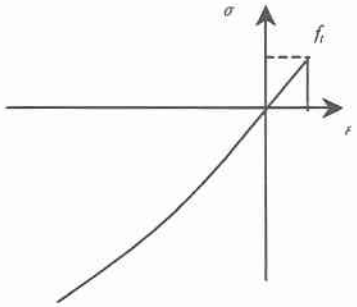

Fig.4 Normal spring model for mortar

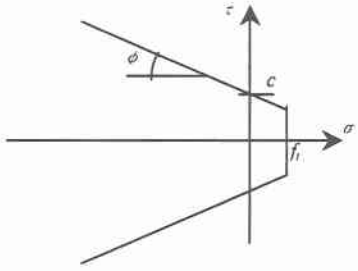

Fig.5 Failure criterion model

Failure criterion for mortal used in the analysis is shown in Fig.5. Coefficients c and ϕ are $3f_t$ and 35°, respectively. Those values were decided based on the previous report[3]. It is assumed in this study that crashing or cracking take place immediately after stresses generated attain the failure criterion and as a result no stresses are developed in the springs.

The following tress-strain relationships of the interface between mortar and aggregate are assumed.

$$\sigma = E\varepsilon$$
$$\tau = G\gamma \qquad (2)$$

Stiffness E and G of interface are given by a weighted average of the material properties in two particles according to their perpendiculars. That is,

$$E = \frac{E_1 h_1 + E_2 h_2}{h_1 + h_2}$$
$$G = \frac{G_1 h_1 + G_2 h_2}{h_1 + h_2} \qquad (3)$$

where subscripts 1 and 2 represent to particles 1 and 2, respectively (Fig.1). The failure criterion shown in Fig.4 is also adapted for interface but different values of c and ϕ are used[4)5)].

In the analysis, only the maximum tensile stress has to be set as a material strength. Considering the effect of stress concentration due to random geometry in analysis, set tensile stress(f_t) is obtained as follows,

$$f_t = 1.2 f_{t\,macro} \qquad (4)$$

where $f_{t\,macro}$ is a tensile stress obtained from pure tensile test.

4. ANALYTICAL RESULTS AND COMPARISON

4.1 MORTAR ANALYSIS

Numerical analysis of uniaxial compressive and tensile tests of mortar model, N30M, is carried out. Analytical model and material properties are shown in Fig.6 and Table1. In the analytical model, the number of mortar element is 3204. Boundaries of top and bottom sides are fixed to lateral direction.

Figures 7 and 8 show predicted stress strain relationship. The maximum stresses observed in the experiment and analysis are shown in Table2. Although it cannot be mentioned whether or not the analysis can simulate the stress-strain curve well because in the experiment the relationship was not recorded, the shape of stress-strain curve are very similar to those obtained by another reserchers[2)6)]. Maximum stresses in the analysis agree well with the experimental results.

Table 1 Material properties

	E (MPa)	ν	set f_t (MPa)
N30M	20090	0.18	3.55

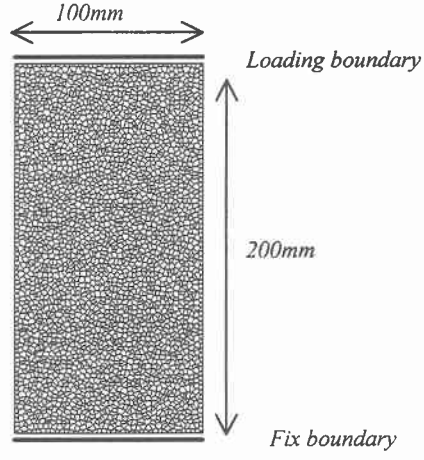

Fig.6 Analytical model of mortar

Table 2 Maximum stress of mortar

	Compressive (MPa)	Tensile (MPa)
N30M- Experiment	27.34	2.96
N30M-Analysis	27.82	2.74

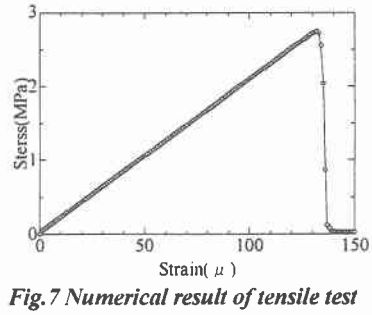

Fig.7 Numerical result of tensile test

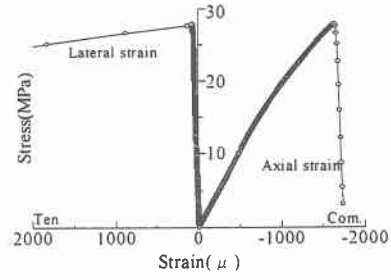

Fig.8 Numerical result of compressive test

In both of analysis for tension and compression (Figs.7 and 8), stress decreases suddenly just after the maximum stress. Before the maximum stress, a few cracks have happened due to stress concentration. But they don't affect macroscopic behavior because released stress at the fracture is carried by another springs around it. At the maximum stress, re-stress distribution and development of major cracks cannot be seen. Cracks did propagate quickly and continuously, typical behavior of brittle failure, because aggregate which disturbs crack propagation did not exist. In this analysis, this fracture process and brittle behavior could simulate.

4.2 CONCRETE MODEL ANALYSIS

Two types of numerical analysis of aggregate-mortar simplified concrete model, N30 and N90, are carried out and compared with experimental results conducted by Kosaka[4]. Experimental and analytical models are shown in Fig.9 a),b). Boundaries of top and bottom sides are not fixed to lateral direction. Geometry between aggregate and mortar is shown in Fig.9 c). Number of element in the analysis is 3245. In the experiment, circular aggregate model is made of mortar so that material model of aggregate is same as mortar in the analysis. Table3 shows material properties of mortar, aggregate and interface. Value of c and ϕ are obtained by the experiment conducted by Kosaka. In N30 model, strength of aggregate model is higher than mortar. On the contrary, mortar has higher strength than aggregate in N90 model. Poisson's ratio could not be obtained from experimental data, so it is set 0.18 in the analysis.

Fig.10 shows experimental and analytical results of N30 and N90 models. In both models, ductile behavior after deviated from elastic stress-displacement relation could not be simulated appropriately. This difference can be explained through the comparison of experimental and analytical results as follows.

In the experiment of N30, bond crack in the interface zone happens at 14MPa for the first obvious damage, because interface is the weakest zone naturally and exposed to stress concentration due to the heterogeneously. And this crack leads to mortar part and makes longitudinal cracks slowly with stress increasing. But these cracks don't through upper and lower side of aggregate because these areas are in compression due to the difference of strength and stiffness. Crashing of mortar in those compressive areas cause the model failure. In the analysis, bond crack happens at 11MPa. Fig.11(N30a)-(N30e) show sifting of stress distribution around the peak stress. Before cracks happen in mortar, bond crack have already existed(Fig.11(N30a)). Leading the cracks from bond crack to axial direction can be seen in Fig.11(N30b)-(N30e). And crack in upper and lower side of aggregate doesn't happen. This fracture process is same as experimental result. But once crack happen in mortar, it leads to longitudinal direction quickly. And model fails due to this longitudinal crack and crashing of mortar in lower part of aggregate. Fig.11(N30f) shows a deformation of model in failure. Main crack passes through the side of aggregate.

In the experiment of N90 model, bond crack happens at 8MPa. Then at 15MPa, aggregate has crashing and mortar has cracks at the almost same time. After that, cracks lead to longitudinal direction in mortar with stress increase until most part of the aggregate is crashed. In case of N90 model, model fails due to the crashing of aggregate. In the analysis, bond crack happens at 7MPa and take same fracture procedure as experiment. Fig.11(N90a)-(N90e) show

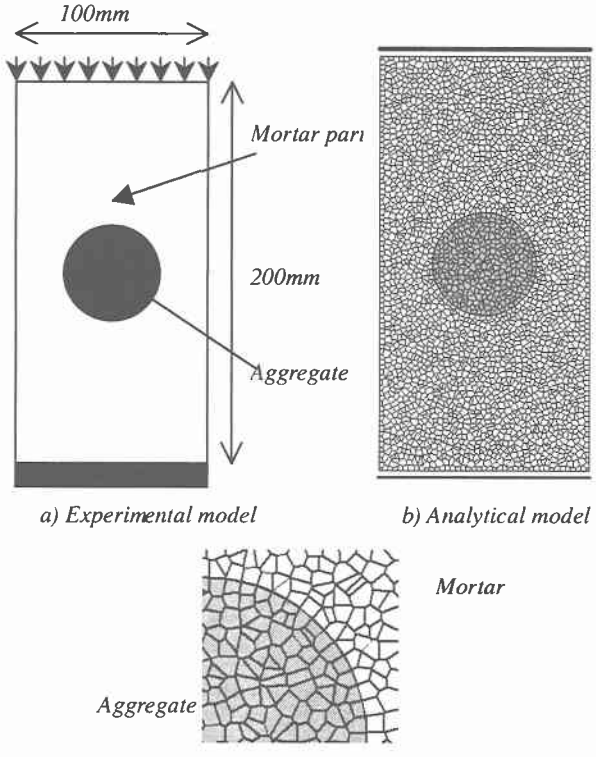

Fig.9 Experimental and analytical model

Table3 Material properties of N30 and N90 model

	N30	N90
Mortar W/C	0.6	0.6
Mortar f'_c (MPa)	27.34	25.48
Mortar f_t (MPa)	2.96	3.28
Mortar E (MPa)	20090	18816
Aggregate W/C	0.3	0.9
Aggregate f'_c (MPa)	54.59	15.78
Aggregate f_t (MPa)	4.37	1.92
Aggregate E (MPa)	24206	10388
Interface c (MPa)	3.14	2.16
Interface ϕ	33°	35°
Interface f_t (MPa)	0.852	0.852

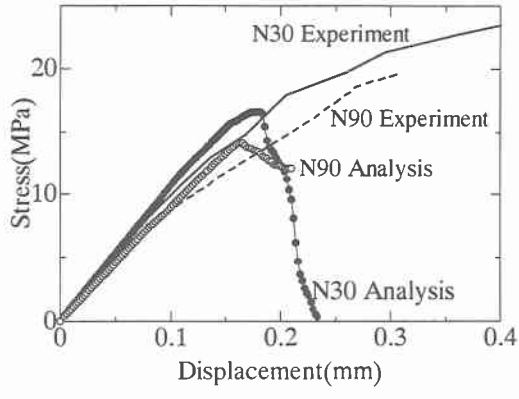

Fig.10 Experimental and analytical results

the sifting of stress distribution around the peak stress. Same as N30 model, bond crack have already existed(Fig.11(N90a)). As shown in Fig.11(N90b)-(N90e), crashing of aggregate and fracture leading to axial direction can be seen. Crashing of aggregate and longitudinal cracks cause the failure of model. Fig.11(N90f) shows deformation in failure. Main crack penetrate the aggregate and aggregate is crashed.

Both in N30 and N90 model's analysis, failure of model is caused by the rapid extension of cracks in the mortar part. Around the peak stress, bond crack and stress concentration generated by the heterogeneously make a new crack which doesn't allow re-stress distribution in mortar. Once it happens, same as the case of mortar analysis, crack propagates quickly and continuously to longitudinal direction. In the experiments, stress increase gradually after happen of main crack because it extends slower than the analysis. This difference brings the different stress-displacement relation in experiment and analysis. Although actual stress-displacement curves couldn't be obtained, the facture procedure and failure deformation of concrete model could be simulated.

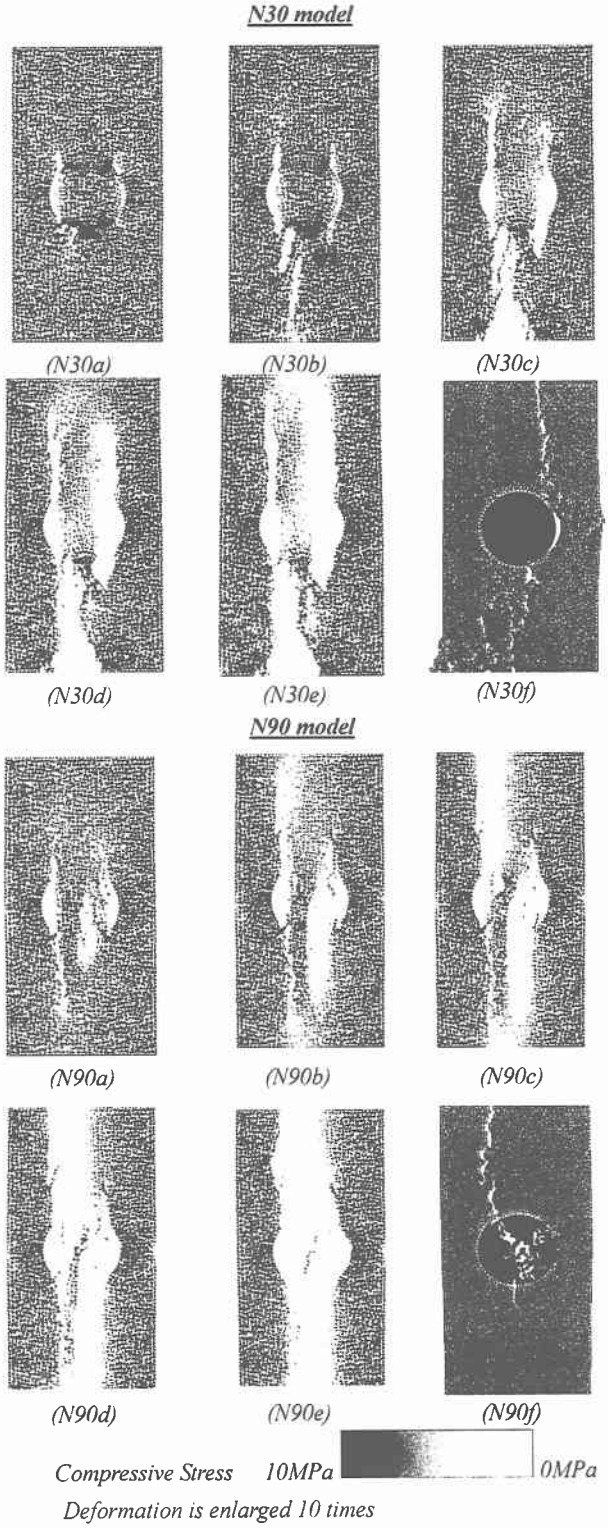

Fig.11 Stress distribution and failure deformation

5. CONCLUSIONS

The followings were derived from the analysis of mortar and concrete model using RBSM.

(1) RBSM developed in this study can simulate fracture process of mortal and concrete model.

(2) The tensile and compressive strengths of mortal can be predicted by RBSM.

(3) RBSM can evaluate quantitatively the influence of aggregate strength on concrete strength and failure mode. However the analysis underestimates the actual strength.

REFERENCES

1) 川井忠彦・竹内則夫共著：コンピューターによる極限解析法シリーズ2，培風館，1990.

2) Harsh, S., Shen, Z. and Darwin, D.: Strain-Rate Sensitive Behavior of Cement Paste and Mortar in Compression, ACI Materials Journal, Sep.-Oct., pp.508-516, 1990.

3) Cowan, H.J., : The strength of plane, reinforced and prestressed concrete under the action of combine stresses, Magazine of Concrete Research, Vol.5, No.14, Dec., pp.75-86, 1954.

4) 小阪義夫，谷川恭雄，太田福男：コンクリートの破壊挙動に及ぼす粗骨材の影響，日本建築学会論文報告集，第228号，2月，pp.1-11, 1975.

5) Taylor, M.A. and Broms, B.B.: Shear Bond Strength Between Coarse Aggregate and Cement Paste or Mortar, ACI Journal, Aug., pp.939-959. 1964

6) 後藤正裕，大塚浩司，守聡史：引張を受けるモルタル表面に発生するマイクロクラック，土木学会第56回年次学術講演会，V-269, pp.538-539, 2001.